Oblique Shock Waves and Shock Reflection *†

Dening Li ‡

Department of Mathematics, West Virginia University, Morgantown, WV 26506, USA

E-mail: li@math.wvu.edu

Abstract

Oblique and conical shock waves are generated as solid projectile flies supersonically, or as a planar shock wave is reflected along a ramp. We study the stability of oblique shock waves for full Euler system of equations in gas-dynamics. The stability criterion is applied to the discussion of regular shock reflection phenomena and the transition of a regular shock reflection to Mach reflection.

1 Introduction

Oblique shock waves are produced as airplane flies supersonically, or as shock waves are reflected at a planar solid surface. With other conditions fixed, the shape of such shock waves at the wings of airplane is determined by the shape of the front edge of the wing. At very small angle θ of a sharp wing edge, the shock front is attached to the wing. The shock front becomes detached as the angle θ increases past a critical angle. Figure 1 shows the profile of an attached shock wave and the flow at a sharp wedge, see [1, 13, 29]. It is of great interest to know the exact angle θ at which an attached shock front transforms into a detached one, since a detached shock front drastically increases resistance to the flight. Mathematically, it requires the

*Mathematics Subject Classification(2000 Revision): Primary 35L65, 35L67; Secondary 76L05.

†Keywords: Euler system, stability, oblique shock wave, regular and Mach shock reflection.

‡supported in part by DoDEPSCOR N000014-02-1-0577 and WVU Faculty Development Fund.

determination of the maximal angle θ_c which would guarantee a stable oblique shock front and for an angle larger than θ_c, the shock front might become detached.

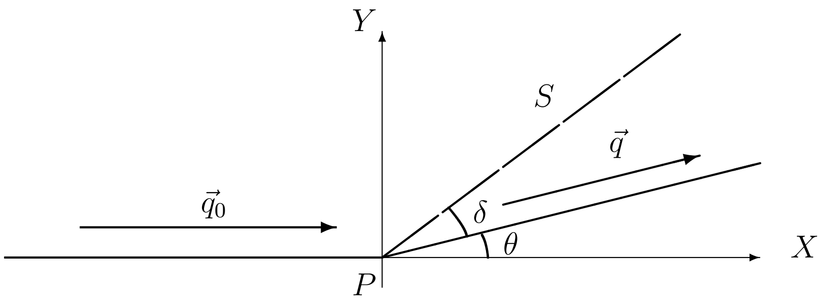

Figure 1: An attached oblique shock wave in supersonic flight

$\vec{q}_0$: incoming upstream velocity;

$\vec{q}$: inflected downstream velocity;

S: attached shock front;

θ: angle between incoming velocity and solid surface;

δ: shock inflection angle.

Oblique shock waves has been studied by many researchers, using theoretical, numerical and experimental tools. Theoretical analysis has been done for various approximate mathematical models. For an irrotational potential flow model, it was studied in [7, 9, 25, 27] for very small incident angle θ. Conical shock waves had been studied in [8]. For an unsteady transonic small disturbance equation in [2]. For the complete Euler system of equations, the non-stationary stability has been studied in [6, 32].

Using an isentropic Euler system model, the stability of oblique shock waves is studied in [19]. A necessary and sufficient condition is established for the linear stability of Kreiss' type [16] under genuine 3-dimensional perturbation. The stability and existence of conical shock waves was established in [11].

However, we know that in gas-dynamics entropy must increase across shock front, the isentropic mathematical model is a good proximation only for very weak shock waves. The optimal condition obtained in [19] for the stability of oblique shock wave is expressed in terms of shock strength which already lies beyond the range of very weak shock. Therefore, for the application in gas-dynamics, it is necessary to derive the stability condition for the full non-isentropic Euler system.

The shock reflection phenomena is closely related to the oblique shock waves. In shock reflection, an incoming planar shock front is reflected along a planar wall. If the incident angle α is very small, then the incident and reflected shock fronts will intersect at a point P on the plane surface. This is called the regular shock reflection. Figure 2 shows the incident and reflected shock waves near their intersection point P on an infinite planar wall.

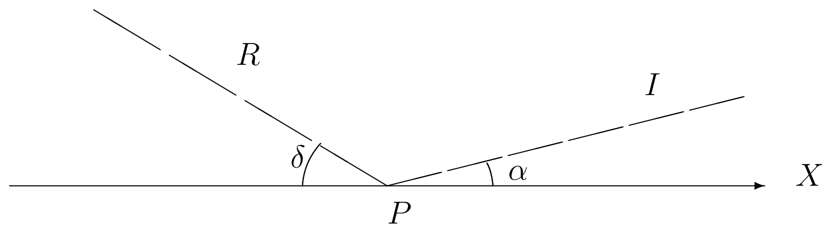

Figure 2: Regular shock reflection at a planar infinite ramp

I: incident shock front;

R: reflected shock front;

α: angle between incident shock front and planar ramp;

δ: angle between reflected shock front and planar ramp.

As incident angle α increases past a critical value, the configuration in Figure 2 will change into a more complicated Mach reflection [13, 15, 29], with a third shock (Mach stem) connecting the intersection point and the plane surface, as well as other features such as vortex sheet. Again, it is of great interest to determine the exact angle α_c at which such transition happens. There are many works on this subject, using various models, see [1, 2, 3, 13, 15, 32, 33], also see [29] for a recent survey on the topic.

The mathematical relations derived from Rankine-Hugoniot conditions on shock fronts prescribe a maximal angle α_m beyond which a regular reflection is simply impossible. However it is observed in experiment that the transition from regular reflection to Mach reflection happens at an angle α_c smaller than α_m, see also [1, 12, 15].

In [29] , concerning this phenomenon it is remarked that “this anticipated transition must be due to some instability, but has not been explained rigorously so far, see [29](§3.1). One of the purpose of this paper is to address this issue and perform a rigorous stability analysis which provides an explanation to this "earlier" transition.

We first derive a sufficient and necessary condition similar to [19] for the oblique shock wave using full non-isentropic Euler system. Then we will apply the result to the study of regular shock reflection and obtain Theorem 3.1. Theorem 3.1 shows that the reflection shock wave fails to satisfy the stability condition at an angle θ_c which is smaller than the angle θ_m predicted from Rankine-Hugoniot condition. This conclusion confirms the observation in physical experiment that, for fixed shock strength, the transition from regular reflection to Mach reflection happens at an angle smaller than θ_m [1, 12, 15, 29]. The result shows that the prediction in [29] is indeed correct.

The paper is arranged as follows. In Section 2, we give the mathematical formulation of the problem and state the main theorem (Theorem 2.1) for oblique shock waves. A comparison discussion is also given in Remark 2.3 about the result in [32]. In Section 3, the main theorem in Section 2 is applied in the analysis of regular shock reflection and obtain Theorem 3.1 regarding its stability and its physical implications. The detailed proof of Theorem 2.1 on the linear stability of oblique shock front is given in section 4.

2 Mathematical formulation and theorems for oblique shock waves

The full Euler system for non-viscous flow in gas-dynamics is the quasi-linear Euler system of equations:

$$\begin{cases} \partial_t \rho + \sum_{j=1}^{3} \partial_{x_j}(\rho v_j) = 0, \\ \partial_t(\rho v_i) + \sum_{j=1}^{3} \partial_{x_j}(\rho v_i v_j + \delta_{ij} p) = 0, \quad i = 1, 2, 3 \\ \partial_t(\rho E) + \sum_{j=1}^{3} \partial_{x_j}(\rho E v_j + p v_j) = 0. \end{cases} \tag{2.1}$$

In (2.1), $(\rho, \mathbf{v})$ are the density and the velocity of the gas particles, $E = e + \frac{1}{2}|\mathbf{v}|^2$ is the total energy, and the pressure $p = p(\rho, E)$ is a known function.

In the region where the solution is smooth, the conservation of total energy in (2.1) can be replaced by the conservation of entropy S [13, 28], and system (2.1) can be replaced by the following system

$$\begin{cases} \partial_t \rho + \sum_{j=1}^{3} \partial_{x_j}(\rho v_j) = 0, \\ \partial_t(\rho v_i) + \sum_{j=1}^{3} \partial_{x_j}(\rho v_i v_j + \delta_{ij} p) = 0, \quad i = 1, 2, 3 \\ \partial_t(\rho S) + \sum_{j=1}^{3} \partial_{x_j}(\rho v_j S) = 0 \end{cases} \tag{2.2}$$

with pressure $p = p(\rho, S)$ satisfying

$$p_\rho > 0, \quad p_{\rho\rho} > 0. \tag{2.3}$$

Shock waves are piece-wise smooth solutions for (2.1) which have a jump discontinuity along a hyper-surface $\phi(t, x) = 0$. On this hyper-surface, the solutions for (2.1) must satisfy the following Rankine-Hugoniot conditions, see [13, 28, 30],

$$\phi_t \begin{bmatrix} \rho \\ \rho v_1 \\ \rho v_2 \\ \rho v_3 \\ \rho E \end{bmatrix} + \phi_{x_1} \begin{bmatrix} \rho v_1 \\ \rho v_1^2 + p \\ \rho v_1 v_2 \\ \rho v_1 v_3 \\ (\rho E + p) v_1 \end{bmatrix} + \phi_{x_2} \begin{bmatrix} \rho v_2 \\ \rho v_1 v_2 \\ \rho v_2^2 + p \\ \rho v_2 v_3 \\ (\rho E + p) v_2 \end{bmatrix} + \phi_{x_3} \begin{bmatrix} \rho v_3 \\ \rho v_1 v_3 \\ \rho v_2 v_3 \\ \rho v_3^2 + p \\ (\rho E + p) v_3 \end{bmatrix} = 0. \tag{2.4}$$

Here $[f] = f_1 - f_0$ denotes the jump difference of f across the shock front $\phi(t, x) = 0$. In this paper, we will use subscript "$_0$" to denote the status on the upstream side (or, ahead) of the shock front and subscript "$_1$" to denote the status on the downstream side (or, behind).

Rankine-Hugoniot condition (2.4) admits many non-physical solutions to (2.1). To single out physical solution, we could impose the stability condition, which argues that for observable physical phenomena, the solution to mathematical model should be stable under small perturbation. In the case of one space dimension, this condition is provided by Lax' shock inequality which demands that a shock wave is linearly stable if and only if the flow is supersonic (relative to the shock front) in front of the shock front and is subsonic (relative to the shock front) behind the shock front, see [13, 30].

In the case of high space dimension, it is shown that Lax' shock inequality also implies the linear stability of the shock front under multi-dimensional perturbation for isentropic polytropic gas[21, 22]. An extra condition on shock strength is needed for general non-isentropic flow, see [21, 22].

Obviously, all multi-dimensional shock waves should satisfy the Lax' shock inequality mentioned above [13, 30]. However, in the study of steady oblique or conical shock waves, the issue is the stability of shock waves with respect to the small perturbation in the incoming supersonic flow or the solid surface. This is the stability independent of time as in [5, **?**], in contrast to the stability studied in [21, 32], and is also different from the study of other unsteady flow, see [2, 4, 20, 25].

Recently, the stability of oblique shock wave under multi-dimensional perturbation in incoming flow was studied in [19] for isentropic Euler system and an optimal condition was derived. In addition to the usual Lax' shock inequality, it was shown in [19] that the downstream supersonic flow and a restriction of shock strength guarantee the stability of oblique shock wave. In particular for polytropic gas, the downstream supersonic flow alone guarantees the stability. Based upon the result, the stability and existence of conical shock waves are established for isentropic Euler system in [10].

In this paper, we study the full Euler system to remove the isentropic restrictions in [19] and [10], and obtain similar optimal conditions for stability of oblique shock waves. The main result on the stability of oblique shock wave is the following theorem.

Theorem 2.1 For three-dimensional Euler system of gas-dynamics (2.1), a steady oblique shock wave is linearly stable with respect to the three dimensional perturbation in the incoming supersonic flow and in the sharp solid surface if

1. The usual entropy condition or its equivalent is satisfied across the shock front. For example, if shock is compressive, i.e., the density increases across the shock front:

$$\rho_1 > \rho_0. \tag{2.5}$$

   Or equivalently, Lax' shock inequality is satisfied.

2. The flow is supersonic behind the shock front

$$|\mathbf{v}| > a. \tag{2.6}$$

3. The shock strength $\rho_1/\rho_0 - 1$ satisfies

$$\left(\frac{v_n}{|\mathbf{v}|}\right)^2 \left(\frac{\rho_1}{\rho_0} - 1\right) < 1. \tag{2.7}$$

   In (2.7), v_n denotes the normal component of the downstream flow velocity $\mathbf{v}$.

The conditions (2.5),(2.6) and (2.7) are also necessary for the linear stability of a plane oblique shock front formed by uniform supersonic incoming flow.

Remark 2.1 The necessity part of the theorem follows from the fact that Kreiss' condition [16] is the necessary and sufficient condition for the well-posedness of the initial-boundary value problem for hyperbolic systems under consideration.

Remark 2.2 It is interesting to compare condition (1.5) with the following conditions in [21] (see (1.17) in [21]):

$$M^2(\rho_1/\rho_0 - 1) < 1, \quad M < 1. \tag{2.8}$$

We notice that (2.7) and (2.8) have very similar forms. The only difference is that the Mach number M in the first relation of (2.8) is replaced here by $v_n/|\mathbf{v}|$ in (2.8). Since Mach number $M < 1$ in (2.8) and $|\mathbf{v}| > a$ in (2.6), we have

$$\frac{v_n}{|\mathbf{v}|} < M.$$

Hence condition (2.7) is weaker than conditions (2.8) in [21].

Despite the apparent similarity, we emphasize that (2.7) in this paper and (2.8) (or (1.17) in [21]) deal with two different types of stability. (2.7) is about the time-independent stability with respect to the perturbation of incoming flow and solid surface, while (2.8) is about the transitional stability with respect to the perturbation of initial data.

In particular, Theorem 2.1 predicts a drastic change in the behavior of oblique shock waves as shock strength increases and the downstream flow becomes subsonic. A similar result was obtained in [19] for isentropic Euler system. Theorem 2.1 confirms that this remains a physically sound criteria for full non-isentropic Euler system where the shock strength may not be small.

To better understand the physical implication of the conditions in Theorem 2.1, let's examine the shock polar in Figure 3, which determine the dependency of downstream velocity $\vec{q}$ upon the angle θ, assuming other parameters unchanged.

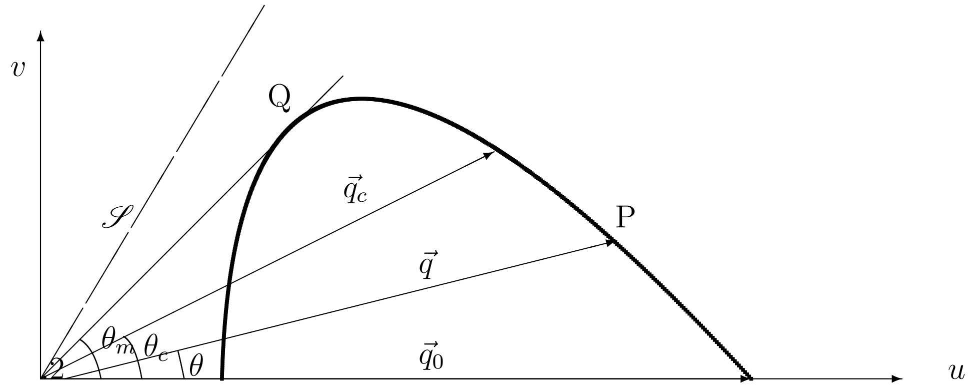

Figure 3: Shock polar determines the downstream velocity $\vec{q}$.

$\vec{q}_0$: incoming upstream velocity;

$\vec{q}$: inflected downstream velocity;

θ: shock inflection angle.

θ_m: the maximal shock inflection angle.

$\vec{q}_c$: the velocity with magnitude of sound speed a.

θ_c: the critical angle for shock stability.

$\mathscr{S}$: shock front;.

In Figure 3, every incident angle θ corresponds two theoretically possible oblique shock waves, with the strong ones being well-known unstable. In this paper, we consider only the "weak" ones, even though they may have large incident angle θ, and with relatively big shock strength. The critical velocity $\vec{q}_c$ has magnitude of sound speed and corresponds to a critical angle θ_c. For all $\theta < \theta_c$, the downstream flow is supersonic ($|\vec{q}| > a$) and the oblique shock wave is linearly stable, and for all $\theta > \theta_c$, the downstream flow is subsonic ($|\vec{q}| < a$) and the linear stability conditions fail. In particular, at the theoretically maximal angle $\theta_m > \theta_c$ (even though their difference is small[1, 15]), the downstream flow is subsonic. Therefore, for all $\theta \in (\theta_c, \theta_m)$, Theorem 2.1 predicts an unstable "weak" oblique shock wave. The angle $\theta_c < \theta_m$ provides a prediction of the exact transition angle from an attached shock front to a detached shock front.

Remark 2.3 A special remark is made here to compare the results obtained in [32] and Theorem 2.1. In [32], the linear stability is studied for oblique shock wave and shock reflection. Under the usual gas state assumptions, e.g., polytropic gas, it is shown in [32] that all weak (relative to strong, but with large incident angle) oblique shock waves (or in the case of shock reflection, weak reflection) are linearly stable, which is obviously different from the conditions in (2.6), (2.7) of Theorem 2.1. This difference comes from the different type of stability.

The stability in [32] is studied with respect to an initial perturbation and hence yields in an initial-boundary problem for a non-stationary linearized system, as in the discussion of [6] and [21]. The condition in Theorem 2.1 is the stability with respect to a perturbation in the incoming flow and reflection surface for a stationary flow. The effect of perturbation is for all time and yields a boundary value problem independent of time. This "global in time" (independent of time) condition actually assumes the local condition (in time) as prerequisite, but imposes extra requirement, which are stronger than the ones in [32] or [21].

This is why the results in [32] did not confirm the experimental phenomena that the actual transition from attached shock wave (or regular reflection) to detached shock wave (or Mach reflection) happens before the theoretically possible maximum angle θ_m, mentioned in [29]. The stronger conditions in (2.6) and (2.7) provide an explanation and point to a transition angle smaller than the one theoretically possible.

3 Analysis of regular shock reflection and its transition to Mach reflection

In this section, we apply Theorem 2.1 to the analysis of regular shock reflection. We consider the planar regular shock reflection along an infinite plane wall, as in Figure 2. Because the stability result in Theorem 2.1 is with respect to three dimensional perturbation, our discussion also applies to the case of a curved shock front along an uneven solid surface. In addition it also applies to the local discussion near the intersection point of a regular reflection along a ramp or wedge.

As in Figure 2, a planar incident shock wave with shock front velocity $\mathbf{v}_0$ is reflected along an infinite wall X and the angle between incident shock front and wall is α, the angle between reflected shock front and wall is δ.

Because the full Euler system of equations is Galilean invariant, if $(\rho, \mathbf{v}, e)$ is a solution, and $\mathbf{U}$ is a constant velocity vector, then $(\rho(x + \mathbf{U}t, t), \mathbf{v}(x + \mathbf{U}t, t), e(x + \mathbf{U}t, t))$ is also a solution. Therefore, in the study of regular planar shock reflection, we can always choose the coordinates moving with the intersection point P in Figure 2, which is moving with constant velocity $\mathbf{U} = |\mathbf{v}_0|/\sin\theta$ along X axis. In this coordinates system, the regular planar reflection at an infinite plane wall becomes stationary. We have the flow velocity in front of incident shock front, the velocity behind the incident shock front but in front of the reflected shock front, and the flow velocity behind the reflected shock, as marked in Figure 4.

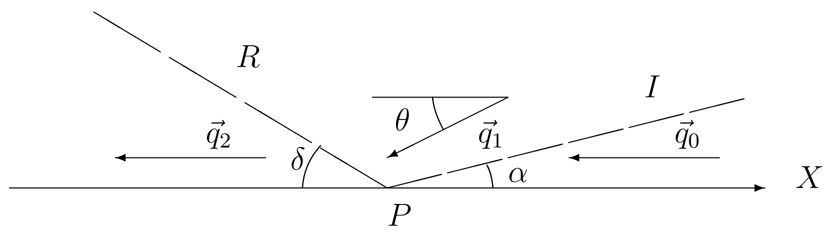

Figure 4: Steady regular shock reflection at an infinite wall

I: incident shock front;

R: reflected shock front;

$\vec{q}_0$: upstream velocity in front of incident shock;

$\vec{q}_1$: inflected flow velocity between incident and reflected shocks;

$\vec{q}_2$: downstream velocity from reflected shock;

α: angle between incident shock front and planar ramp;

δ: angle between reflected shock front and planar ramp.

θ: inflection angle between $\vec{q}_1$ and planar ramp.

From the coordinates frame choice, it is obvious that velocity vector $|\vec{q}_0| = |\mathbf{v}_0|/\sin\alpha$. In the study of shock reflection, the status of the flow on either side of the incident shock front I are given, i.e., the status of the flow region of $\vec{q}_0$ and $\vec{q}_1$ are given. The reflected shock front R, as well as the flow status in its downstream region need to be determined. It has been known [13, 29, 32] the downstream status is uniquely determined by a relation derived from Rankine-Hugoniot conditions on the incident and reflected shock fronts. For a given shock strength of I, the downstream status is uniquely determined by in incident angle α. Indeed, the incident angle α determines the slope of the vector $\vec{q}_1$ and hence θ.

From the point view of the reflected shock front R, θ in Figure 4 is nothing but the inflection angle θ in case of oblique shock wave, in Figure 1 and Figure 3. Therefore, the study of reflected shock front R is the same as the study of an oblique shock wave generated by an incoming flow $\vec{q}_1$ by an inflection angle θ. Consequently, we can apply the results derived in Theorem 2.1 to the shock reflection study and obtain the following theorem.

Theorem 3.1 For three-dimensional Euler system of gas-dynamics (2.1), a steady regular planar shock reflection is linearly stable with respect to the three dimensional perturbation in the incident shock front I and in the solid surface if

1. The usual entropy condition or its equivalent is satisfied across the shock front. For example, if shock is compressive, or equivalently, Lax' shock inequality is satisfied.

2. The flow is supersonic downstream from the reflected shock front R

$$|\vec{q}_2| > a. \tag{3.1}$$

3. The shock strength $\rho_2/\rho_1 - 1$ satisfies

$$\left(\frac{q_n}{|\vec{q}_2|}\right)^2 \left(\frac{\rho_2}{\rho_1} - 1\right) < 1. \tag{3.2}$$

   Here q_n denotes the component of the flow velocity $\vec{q}_2$ normal to the reflected shock front R.

The above conditions are also necessary for the linear stability of a planar regular shock reflection formed by a uniform incident along an infinite planar wall.

We now turn to the shock polar in Figure 3 to see the physical implications of Theorem 3.1, especially in relation to the transition of a regular shock reflection in Figure 2 to a Mach reflection. It is well observed in physical experiment that with fixed strength of the incident shock front I, if the incident angle α is small, then a regular reflection pattern as shown in Figure 2 can be observed. As α increases, the angle θ also increases, and a similar pattern will persist until α reaches a critical value α_c (hence θ reaches a critical value θ_c) beyond which the pattern of shock fronts in Figure 2 is no more valid and the configuration changes into the Mach reflection, with the intersection point P is lifted from the wall and is connected to the wall by an addition shock front called Mach stem, as well as with the appearance of a slip line or even more complicated features, see [13, 15, 29].

It is of great interest to understand the critical angle θ_c (and hence α_c) at which the transition from a regular reflection to Mach reflection happens, and this has been the topic of many research papers. As in the case of oblique shock waves, the shock relations derived from Rankine-Hugoniot conditions prescribe a mathematically maximal angle θ_m. From purely mathematical point of view, the regular reflection could happen up to the angle θ_m, but experiment shows that regular reflection transits to Mach reflection at a critical angle θ_c exactly smaller than θ_m shown in the shock polar in Figure 3.

In [15], it has been argued from an information criteria that Mach reflection is not possible for supersonic downstream flow, i.e., Mach reflection requires that $\theta > \theta_a$ with θ_a denoting the angle corresponding to sonic downstream flow.

On the other hand, in all previous studies it has been shown with mathematical rigor only that the regular reflection is stable for small incident angel α (hence small θ_1).

Theorem 3.1 concludes with mathematical rigor, that if the downstream flow is supersonic (i.e., (3.1) is satisfied), then the regular reflection pattern is stable with respect to 3-dimensional perturbation for moderate shock strength (i.e., (3.2) is automatically satisfied). This confirms the conclusion in [15] based upon the physical information criteria.

In addition, since the condition in Theorem 3.1 is a necessary and sufficient condition for uniform planar shock and wall, hence the subsonic downstream flow implies the onset of instability, consequently provides the hint that the regular reflection pattern in Figure 2 could not be preserved and observed, unless some extra conditions are imposed in the far fields of downstream flow, such as the ones in [5] where transonic shock waves are studied.

In conclusion, we believe that Theorem 3.1 predicts the transition angle θ_c from regular reflection to Mach reflection. It should happen exactly at the critical angle $\theta_c = \theta_a$ which corresponding to sonic downstream flow.

4 Proof of Theorem 2.1

Because of the micro-local nature of Kreiss' conditions for hyperbolic boundary value problems, we need only to consider the linear stability of a uniform oblique shock wave produced by a wedge with plane surface. For simplicity, we choose the coordinate system (x_1, x_2, x_3) such that (see Figure 5)

- The solid wing surface is the plane $x_3 = 0$;
- The downstream flow behind the oblique shock front is in the positive x_1 direction;
- The angle between the solid wing surface and oblique shock front is δ;
- The angle between the incoming supersonic flow and the solid wing surface is θ.

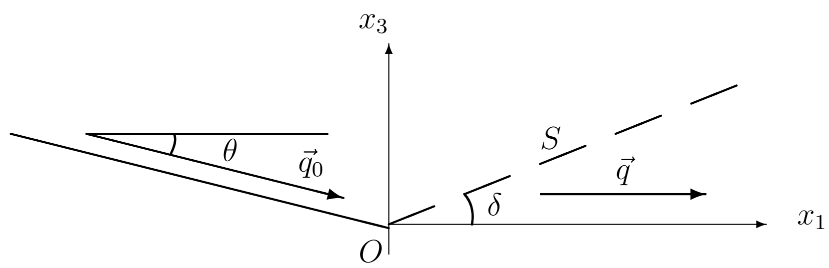

Figure 5: An attached oblique shock wave in supersonic flight

$\vec{q}_0$: incoming upstream velocity;
$\vec{q}$: inflected downstream velocity;
S: attached shock front;
θ: angle between incoming velocity and solid surface;
δ: shock inflection angle.

Consider a small perturbation in the solid surface $x_3 = 0$, as well as in the uniform incoming supersonic steady flow. The perturbed solid surface is $x_3 = b(x_1, x_2)$ with $b(0,0) = b_{x_1}(0,0) = b_{x_2}(0,0) = 0$, the downstream flow after shock front should be close to the direction of positive x_1-axis. The perturbed oblique shock front is described by $x_3 = s(x_1, x_2)$ such that $s(0,0) = s_{x_2}(0,0) = 0$ and $s_{x_1} \sim \lambda = \tan\delta > 0$. Obviously we have $b(x_1, x_2) < s(x_1, x_2)$ for all (x_1, x_2).

In the region $b(x_1, x_2) < x_3 < s(x_1, x_2)$, the steady flow is smooth. Hence Euler system (2.1) can be replaced by (2.2) and we have

$$\begin{cases} \sum_{j=1}^{3} \partial_{x_j}(\rho v_j) = 0, \\ \sum_{j=1}^{3} \partial_{x_j}(\rho v_i v_j + \delta_{ij} p) = 0, \quad i = 1, 2, 3; \\ \sum_{j=1}^{3} \partial_{x_j}(\rho v_j S) = 0. \end{cases} \tag{4.1}$$

On the shock front $x_3 = s(x_1, x_2)$, Rankine-Hugoniot condition (2.4) becomes

$$s_{x_1} \begin{bmatrix} \rho v_1 \\ \rho v_1^2 + p \\ \rho v_1 v_2 \\ \rho v_1 v_3 \\ (\rho E + p) v_1 \end{bmatrix} + s_{x_2} \begin{bmatrix} \rho v_2 \\ \rho v_1 v_2 \\ \rho v_2^2 + p \\ \rho v_2 v_3 \\ (\rho E + p) v_2 \end{bmatrix} - \begin{bmatrix} \rho v_3 \\ \rho v_1 v_3 \\ \rho v_2 v_3 \\ \rho v_3^2 + p \\ (\rho E + p) v_3 \end{bmatrix} = 0. \tag{4.2}$$

On the solid surface $x_3 = b(x_1, x_2)$ of the wing, the flow should be tangential to the surface and we have the boundary condition

$$v_1 \frac{\partial b}{\partial x_1} + v_2 \frac{\partial b}{\partial x_2} - v_3 = 0. \tag{4.3}$$

The study of oblique shock wave consists of investigating the system (4.1) with the boundary conditions (4.2) and (4.3).

System (4.1) can be written as a symmetric system for the unknown vector function $U = (p, v_1, v_2, v_3, S)^T$ in $b(x_1, x_2) < x_3 < s(x_1, x_2)$:

$$A_1 \partial_{x_1} U + A_2 \partial_{x_2} U + A_3 \partial_{x_3} U = 0 \tag{4.4}$$

where

$$A_1 = \begin{pmatrix} \frac{v_1}{a^2\rho} & 1 & 0 & 0 & 0 \\ 1 & \rho v_1 & 0 & 0 & 0 \\ 0 & 0 & \rho v_1 & 0 & 0 \\ 0 & 0 & 0 & \rho v_1 & 0 \\ 0 & 0 & 0 & 0 & \rho v_1 \end{pmatrix}, \quad A_2 = \begin{pmatrix} \frac{v_2}{a^2\rho} & 0 & 1 & 0 & 0 \\ 0 & \rho v_2 & 0 & 0 & 0 \\ 1 & 0 & \rho v_2 & 0 & 0 \\ 0 & 0 & 0 & \rho v_2 & 0 \\ 0 & 0 & 0 & 0 & \rho v_2 \end{pmatrix}$$

$$A_3 = \begin{pmatrix} \frac{v_3}{a^2\rho} & 0 & 0 & 1 & 0 \\ 0 & \rho v_3 & 0 & 0 & 0 \\ 0 & 0 & \rho v_3 & 0 & 0 \\ 1 & 0 & 0 & \rho v_3 & 0 \\ 0 & 0 & 0 & 0 & \rho v_3 \end{pmatrix}. \tag{4.5}$$

Under the downstream supersonic flow assumption, we have $v_1^2 > a^2$ and it is readily checked that matrix A_1 is positively definite. Therefore (4.4) is a hyperbolic symmetric system [14] with x_1 being the time-like direction.

On the fixed boundary $x_3 = b(x_1, x_2)$, the boundary matrix

$$A_3 - A_1 b_{x_1} - A_2 b_{x_2} = \begin{pmatrix} 0 & -b_{x_1} & -b_{x_2} & 1 & 0 \\ -b_{x_1} & 0 & 0 & 0 & 0 \\ -b_{x_2} & 0 & 0 & 0 & 0 \\ 1 & 0 & 0 & 0 & 0 \\ 0 & 0 & 0 & 0 & 0 \end{pmatrix}. \tag{4.6}$$

It is readily checked that the boundary condition (4.3) is admissible with respect to system (4.4) in the sense of Friedrichs [14, 17, 18, 26] and there is a corresponding energy estimate for the linearized problem. Therefore, we need only to study the linearized problem for (4.1) (or (4.4)) and (4.2) near the shock front.

We perform the following coordinates transform to fix the shock front $x_3 = s(x_1, x_2)$:

$$x_1' = x_1, \quad x_2' = x_2, \quad x_3' = x_3 - s(x_1, x_2). \tag{4.7}$$

In the coordinates (x_1', x_2', x_3'), the shock front is $x_3' = 0$ and the shock front position $x_3 = s(x_1, x_2)$ becomes an unknown function, coupled with U. To simplify the notation, we will denote the new coordinates in the following again as (x_1, x_2, x_3). The system (4.4) in the new coordinates becomes

$$A_1 \partial_{x_1} U + A_2 \partial_{x_2} U + \tilde{A}_3 \partial_{x_3} U = 0 \tag{4.8}$$

where $\tilde{A}_3 = A_3 - s_{x_1}A_1 - s_{x_2}A_2$. The Rankine-Hugoniot boundary condition (4.2) is now defined on $x_3 = 0$ and takes the same form:

$$s_{x_1}\begin{bmatrix} \rho v_1 \\ \rho v_1^2 + p \\ \rho v_1 v_2 \\ \rho v_1 v_3 \\ (\rho E + p)v_1 \end{bmatrix} + s_{x_2}\begin{bmatrix} \rho v_2 \\ \rho v_1 v_2 \\ \rho v_2^2 + p \\ \rho v_2 v_3 \\ (\rho E + p)v_2 \end{bmatrix} - \begin{bmatrix} \rho v_3 \\ \rho v_1 v_3 \\ \rho v_2 v_3 \\ \rho v_3^2 + p \\ (\rho E + p)v_3 \end{bmatrix} = 0. \tag{4.9}$$

System (4.8) with boundary condition (4.9) is a coupled boundary value problem for unknown variables (U, s) with U defined in $x_3 < 0$ and s being a function of (x_1, x_2). To examine Kreiss' condition, we need to study the linear stability of (4.8)(4.9) near the uniform oblique shock front with downstream flow:

$$U_1 = (p, v_1, 0, 0, S), \quad s = \lambda x_1. \tag{4.10}$$

where $\lambda = \tan\delta$ with δ being the angle between solid surface and oblique shock front. Under the assumptions in Theorem 2.1, behind the shock front we have

$$v_1 > a, \quad v_n \equiv v_1 \sin\delta < a \tag{4.11}$$

where v_n is the flow velocity component normal to the shock front.

Let (V, σ) be the small perturbation of (U, s) with $V = (\dot{p}, \dot{v}_1, \dot{v}_2, \dot{v}_3, \dot{S})$. The linearization of (4.8) is the following linear system

$$A_{10}\partial_{x_1}V + A_{20}\partial_{x_2}V + A_{30}\partial_{x_3}V + C_1\sigma_{x_1} + C_2\sigma_{x_2} + C_3V = f. \tag{4.12}$$

Here $A_{10} = A_1$ in (4.5) and

$$A_{20} = \begin{pmatrix} 0 & 0 & 1 & 0 & 0 \\ 0 & 0 & 0 & 0 & 0 \\ 1 & 0 & 0 & 0 & 0 \\ 0 & 0 & 0 & 0 & 0 \\ 0 & 0 & 0 & 0 & 0 \end{pmatrix}, \tag{4.13}$$

$$A_{30} = \begin{pmatrix} -a^{-2}\rho^{-1}\lambda v_1 & -\lambda & 0 & 1 & 0 \\ -\lambda & -\lambda\rho v_1 & 0 & 0 & 0 \\ 0 & 0 & -\lambda\rho v_1 & 0 & 0 \\ 1 & 0 & 0 & -\lambda\rho v_1 & 0 \\ 0 & 0 & 0 & 0 & -\lambda\rho v_1 \end{pmatrix}. \tag{4.14}$$

The explicit forms of C_1, C_2 and C_3 are of no consequence in the following discussion.

Direct computation shows that A_{30} has one negative triple eigenvalue $-\lambda\rho v_1$ and other two eigenvalues satisfying the quadratic equation

$$y^2 + \lambda v_1 \left(\rho + \frac{1}{a^2\rho}\right) y - \frac{1}{a^2}\left(a^2 + a^2\lambda^2 - \lambda^2 v_1^2\right) = 0. \tag{4.15}$$

Lax' shock inequality implies that the normal velocity behind the shock front is subsonic, hence $a^2 - v_n^2 > 0$. The quantity $(a^2 + a^2\lambda^2 - \lambda^2 v_1^2)$ in (4.15) will be used often later and will be denoted as

$$\nu^2 = (a^2 + a^2\lambda^2 - \lambda^2 v_1^2) = (1+\lambda^2)(a^2 - v_n^2) > 0. \tag{4.16}$$

Therefore (4.15) has one positive root and one negative root and matrix A_{30} has four negative eigenvalues and one positive eigenvalue.

Denote U_0, U_1 the upstream and downstream state of shock front respectively. To simplify the notation, we drop the subscription "$_1$" when there is no confusion:

$$U_0 = (p_0, v_{10}, 0, v_{30}, S_0), \quad U_1 = (p_1, v_{11}, 0, 0, S_1) \equiv (p, v_1, 0, 0, S).$$

The linearization of boundary condition (4.9) has the form

$$\mathbf{a}_1 \partial_{x_1}\sigma + \mathbf{a}_2 \partial_{x_2}\sigma + BV = g. \tag{4.17}$$

Here $\mathbf{a}_1$ and $\mathbf{a}_2$ are vectors in $\mathbb{R}^5$:

$$\mathbf{a}_1 = \begin{pmatrix} a_{11} \\ a_{12} \\ 0 \\ a_{14} \\ a_{15} \end{pmatrix} \equiv \begin{pmatrix} \rho v_1 - \rho_0 v_{10} \\ \rho v_1^2 + p - \rho_0 v_{10}^2 - p_0 \\ 0 \\ -\rho_0 v_{10} v_{30} \\ (\rho E + p) v_1 - (\rho_0 E_0 + p_0) v_{10} \end{pmatrix}, \quad \mathbf{a}_2 = \begin{pmatrix} 0 \\ 0 \\ p - p_0 \\ 0 \\ 0 \end{pmatrix}, \tag{4.18}$$

and B is a 5×5 matrix defined by the following differential evaluated at uniform oblique shock front:

$$BdU \equiv \lambda d \begin{pmatrix} \rho v_1 \\ \rho v_1^2 + p \\ \rho v_1 v_2 \\ \rho v_1 v_3 \\ (\rho E + p) v_1 \end{pmatrix} - d \begin{pmatrix} \rho v_3 \\ \rho v_1 v_3 \\ \rho v_2 v_3 \\ \rho v_3^2 + p \\ (\rho E + p) v_3 \end{pmatrix}. \tag{4.19}$$

Denote

$$\|u\|_\eta = \left(\int_{-\infty}^{\infty}\int_{-\infty}^{\infty}\int_{0}^{\infty} e^{-2\eta x_1}|u(x)|^2 dx_3\, dx_2\, dx_1\right)^{\frac{1}{2}},$$

$$|u|_\eta = \left(\int_{-\infty}^{\infty}\int_{-\infty}^{\infty} e^{-2\eta x_1}|u(x_1,x_2,0)|^2 dx_2\, dx_1\right)^{\frac{1}{2}},$$

$$|u|_{1,\eta} = \left(\sum_{t_0+t_1+t_2\le 1}\int_{-\infty}^{\infty}\int_{-\infty}^{\infty} \eta^{2t_0} e^{-2\eta x_1}|\partial_{x_1}^{t_1}\partial_{x_2}^{t_2} u(x_1,x_2,0)|^2 dx_2\, dx_1\right)^{\frac{1}{2}}.$$

The boundary value problem (4.12)(4.17) is said to be well-posed and the steady oblique shock front is linearly stable if there is an $\eta_0 > 0$ and a constant C_0 such that

$$\eta\|V\|_\eta^2 + |V|_\eta^2 + |\sigma|_{1,\eta}^2 \le C_0\left(\frac{1}{\eta}\|f\|_\eta^2 + |g|_\eta^2\right) \tag{4.20}$$

for all solutions $(V,\sigma) \in C_0^\infty(\mathbb{R}^1 \times \mathbb{R}^2) \times C_1^\infty(\mathbb{R}^2)$ of (4.1)(4.2) and for all $\eta \ge \eta_0$.

Denote

$$\tilde{\mathbf{a}}(s, i\omega) = s\mathbf{a}_1 + i\omega\mathbf{a}_2, \tag{4.21}$$

then we have from (4.18),

$$\tilde{\mathbf{a}}(s, i\omega) \neq 0 \ \text{ on } \ |s|^2 + |\omega|^2 = 1. \tag{4.22}$$

Let Π be the projector in C^5 in the direction of vector $\tilde{\mathbf{a}}(s, i\omega)$, then

$$p(s, i\omega) = (I - \Pi)B \tag{4.23}$$

is a 5×5 matrix of rank 4, with elements being symbols in S^0, i.e., functions of zero-degree homogeneous in $(s, i\omega)$, see [21]. The study of linear stability of oblique shock front under perturbation is reduced to the investigation of Kreiss' condition for the following boundary value problem

$$\begin{cases} A_1\partial_{x_1}V + A_{20}\partial_{x_2}V + A_{30}\partial_{x_3}V = f_1 \ \text{ in } \ x_3 < 0, \\ PV = g_1 \ \text{ on } \ x_3 = 0. \end{cases} \tag{4.24}$$

Here P is the zero-order pseudo-differential operator [31] with symbol $p(s, i\omega)$ in (4.23).

The stability result of this section is the following theorem about the well-posedness of (4.24).

Theorem 4.1 The linear boundary value problem (4.24), describing the linear stability of steady oblique plane shock front, is well-posed in the sense of Kreiss [16, 23, 24] if

1. $\rho > \rho_0$, i.e., the shock is compressive. This is the usual entropy condition.
2. The downstream flow is supersonic, i.e., $v_1 > a_-$. This guarantees the hyperbolicity of system in (4.24).
3. The following condition on the strength of shock front $\rho/\rho_0 - 1$ is satisfied
$$\left(\frac{v_n}{|\mathbf{v}|}\right)^2 \left(\frac{\rho}{\rho_0} - 1\right) < 1. \tag{4.25}$$

The above conditions are also necessary for the problem (4.24) with constant coefficients.

To prove Theorem 4.1 (and hence Theorem 2.1), we construct the matrix $M(s, i\omega)$ as in [16, 23, 24]

$$M(s, i\omega) = -A_{30}^{-1}(sA_1 + i\omega A_{20}). \tag{4.26}$$

We have

$$sA_1 + i\omega A_{20} = \begin{pmatrix} \frac{sv_1}{a^2\rho} & s & i\omega & 0 & 0 \\ s & s\rho v_1 & 0 & 0 & 0 \\ i\omega & 0 & s\rho v_1 & 0 & 0 \\ 0 & 0 & 0 & s\rho v_1 & 0 \\ 0 & 0 & 0 & 0 & s\rho v_1 \end{pmatrix}$$

and

$$A_{30}^{-1} = \frac{(\lambda\rho v_1)^2}{|D|} \begin{pmatrix} (\lambda\rho v_1)^2 & -\lambda^2\rho v_1 & 0 & \lambda\rho v_1 & 0 \\ -\lambda^2\rho v_1 & \frac{\lambda^2 v_1^2}{a^2} - 1 & 0 & -\lambda & 0 \\ 0 & 0 & -\nu^2/a^2 & 0 & 0 \\ \lambda\rho v_1 & -\lambda & 0 & \lambda^2(\frac{v_1^2}{a^2} - 1) & 0 \\ 0 & 0 & 0 & 0 & -\nu^2/a^2 \end{pmatrix},$$

where $|D| = (\lambda\rho v_1)^3\nu^2/a^2 > 0$ is the determinant of A_{30} and

$$\nu^2 = (a^2 + a^2\lambda^2 - \lambda^2 v_1^2) = (1 + \lambda^2)(a^2 - v_n^2) > 0.$$

Consider the eigenvalue and eigenvectors of matrix $N(s, i\omega)$:

$$N(s, i\omega) \equiv \frac{|D|}{(\rho\lambda v_1)^2} M(s, i\omega) \tag{4.27}$$

which has the following expression by straightforward computation:

$$N(s, i\omega) = \begin{pmatrix} s\lambda^2\rho v_1(1-\frac{v_1^2}{a^2}) & 0 & -i\omega(\lambda\rho v_1)^2 & -s\lambda(\rho v_1)^2 & 0 \\ s & s\rho v_1\nu^2/a^2 & i\omega\lambda^2\rho v_1 & s\lambda\rho v_1 & 0 \\ i\omega\nu^2/a^2 & 0 & s\rho v_1\nu^2/a^2 & 0 & 0 \\ s\lambda(1-\frac{v_1^2}{a^2}) & 0 & -i\omega\lambda\rho v_1 & s\lambda^2\rho v_1(1-\frac{v_1^2}{a^2}) & 0 \\ 0 & 0 & 0 & 0 & s\rho v_1\nu^2/a^2 \end{pmatrix}.$$

Beside the obvious double eigenvalue $\xi_1 = s\rho v_1\nu^2/a^2$, other eigenvalues are roots of

$$\det \begin{vmatrix} s\lambda^2\rho v_1(1-\frac{v_1^2}{a^2}) - \xi & -i\omega(\lambda\rho v_1)^2 & -s\lambda(\rho v_1)^2 \\ i\omega\nu^2/a^2 & s\rho v_1\nu^2/a^2 - \xi & 0 \\ s\lambda(1-\frac{v_1^2}{a^2}) & -i\omega\lambda\rho v_1 & s\lambda^2\rho v_1(1-\frac{v_1^2}{a^2}) - \xi \end{vmatrix} = 0.$$

Hence the five eigenvalues for $N(s, i\omega)$ are

$$\begin{cases} \xi_1 = \xi_2 = \xi_3 = s\rho v_1\nu^2/a^2, \\ \xi_{4,5} = s\lambda^2\rho v_1(1-\frac{v_1^2}{a^2}) \pm \lambda\rho v_1 a^{-1}\sqrt{s^2(v_1^2-a^2)+\omega^2\nu^2}. \end{cases} \tag{4.28}$$

By $\nu^2 = a^2 + \lambda^2 a^2 - \lambda^2 v_1^2 > 0$, we have

$$(\lambda\rho v_1 a^{-1})^2(v_1^2 - a^2) > (\lambda^2\rho v_1)^2\left(\frac{v_1^2}{a^2} - 1\right)^2.$$

For $\eta = \text{Re}s > 0$, one of $\xi_{4,5}$ has positive real part and one has negative real part in (4.28). Consequently $N(s, i\omega)$ has four eigenvalues with positive real parts and one with negative real part when $\eta > 0$.

For the eigenvalues $\xi_1, \xi_2, \xi_3, \xi_4$ which have positive real parts when $\eta > 0$, we compute the corresponding eigenvectors or generalized eigenvectors for $N(s, i\omega)$.

For the triple eigenvalue $\xi_1 = \xi_2 = \xi_3$, there are three linearly independent eigenvectors:

$$\begin{cases} \alpha_1 = (0, 1, 0, 0, 0)^T, \\ \alpha_2 = (0, 0, s, -i\omega\lambda, 0)^T, \\ \alpha_3 = (0, 0, 0, 0, 1)^T \end{cases} \tag{4.29}$$

Since

$$s\lambda^2\rho v_1\left(1-\frac{v_1^2}{a^2}\right)-\xi_4=-\lambda\rho v_1 a^{-1}\mu,\ \ s\rho v_1\nu^2/a^2-\xi_4=\rho v_1(s-\lambda a^{-1}\mu),$$

the eigenvector α_4 corresponding to the eigenvalue ξ_4 is parallel to

$$\alpha_4=(-\rho v_1(s-\lambda a^{-1}\mu), s-\lambda a^{-1}\mu, i\omega\nu^2/a^2, a^{-1}\mu-s\lambda(v_1^2/a^2-1), 0)^T. \tag{4.30}$$

where

$$\mu\equiv\sqrt{s^2(v_1^2-a^2)+\omega^2\nu^2}. \tag{4.31}$$

The four eigenvectors $\alpha_1,\alpha_2,\alpha_3$ and α_4 are linearly independent at $s\neq\lambda a^{-1}\mu$.

At $s=\lambda a^{-1}\mu$, we have $s^2=\lambda^2\omega^2$ and $\xi_1=\xi_2=\xi_3=\xi_4$. α_4 is parallel to $(0,0,i\omega,-a^{-1}\mu,0)^T$ which is parallel to α_2 at $s=\lambda a^{-1}\mu$. A generalized eigenvector needs to be computed.

4.1 Simplify (4.17)

The Kreiss' condition for (4.24) requires that five vectors $(B\alpha_1, B\alpha_2, B\alpha_3, B\alpha_4)$ and $s\mathbf{a}_1+i\omega\mathbf{a}_2$ are linearly independent on $|s|^2+|\omega|^2=1,\ \eta\geq 0$.

We first simplify (4.17) by elementary row operation. Consider

$$\begin{pmatrix} sa_{11}\\ sa_{12}\\ i\omega a_{23}\\ sa_{14}\\ sa_{15}\end{pmatrix}+\lambda\begin{pmatrix} d(\rho v_1)\\ d(\rho v_1^2+p)\\ d(\rho v_1v_2)\\ d(\rho v_1 v_3)\\ d(\rho v_1E+pv_1)\end{pmatrix}-\begin{pmatrix} d(\rho v_3)\\ d(\rho v_1v_3)\\ d(\rho v_2v_3)\\ d(\rho v_3^2+p)\\ d(\rho v_3E+pv_3)\end{pmatrix}. \tag{4.32}$$

Noticing that the linearization is at the uniform oblique shock front, we have

$$\begin{pmatrix} sa_{11}\\ sa_{12}\\ i\omega a_{23}\\ sa_{14}\\ s(a_{15}-Ea_{11})\end{pmatrix}+\lambda\begin{pmatrix} d(\rho v_1)\\ d(\rho v_1^2+p)\\ \rho v_1dv_2\\ \rho v_1 dv_3\\ \rho v_1dE+d(pv_1)\end{pmatrix}-\begin{pmatrix} \rho dv_3\\ \rho v_1dv_3\\ 0\\ dp\\ pdv_3\end{pmatrix}.$$

and

$$\begin{pmatrix} sa_{11}\\ s(a_{12}-v_1a_{11})\\ i\omega a_{23}\\ sa_{14}\\ s(a_{15}-Ea_{11})\end{pmatrix}+\lambda\begin{pmatrix} d(\rho v_1)\\ \rho v_1dv_1+dp\\ \rho v_1dv_2\\ \rho v_1 dv_3\\ \rho v_1dE+d(pv_1)\end{pmatrix}-\begin{pmatrix} \rho dv_3\\ 0\\ 0\\ dp\\ pdv_3\end{pmatrix}.$$

Since $dE = de + v_1 dv_1$, we have

$$\begin{pmatrix} sa_{11} \\ s(a_{12} - v_1 a_{11}) \\ i\omega a_{23} \\ sa_{14} \\ s(a_{15} - (E - v_1^2)a_{11} - v_1 a_{12}) \end{pmatrix} + \lambda \begin{pmatrix} d(\rho v_1) \\ \rho v_1 dv_1 + dp \\ \rho v_1 dv_2 \\ \rho v_1 dv_3 \\ \rho v_1 de + p dv_1 \end{pmatrix} - \begin{pmatrix} \rho dv_3 \\ 0 \\ 0 \\ dp \\ p dv_3 \end{pmatrix}.$$

Multiply first row by $-p/\rho$ and add to the fifth row, we obtain

$$\begin{pmatrix} sa_{11} \\ s(a_{12} - v_1 a_{11}) \\ i\omega a_{23} \\ sa_{14} \\ s(a_{15} - (E - v_1^2 + p/\rho)a_{11} - v_1 a_{12}) \end{pmatrix} + \lambda \begin{pmatrix} d(\rho v_1) \\ \rho v_1 dv_1 + dp \\ \rho v_1 dv_2 \\ \rho v_1 dv_3 \\ \rho v_1 (de - p/\rho^2 d\rho) \end{pmatrix} - \begin{pmatrix} \rho dv_3 \\ 0 \\ 0 \\ dp \\ 0 \end{pmatrix}.$$

Using $de = TdS - pd\tau$, $(\tau = 1/\rho)$, we have

$$\begin{pmatrix} sa_{11} \\ s(a_{12} - v_1 a_{11}) \\ i\omega a_{23} \\ sa_{14} \\ s(a_{15} - (E - v_1^2 + p/\rho)a_{11} - v_1 a_{12}) \end{pmatrix} + \lambda \begin{pmatrix} d(\rho v_1) \\ \rho v_1 dv_1 + dp \\ \rho v_1 dv_2 \\ \rho v_1 dv_3 \\ \rho v_1 T dS \end{pmatrix} - \begin{pmatrix} \rho dv_3 \\ 0 \\ 0 \\ dp \\ 0 \end{pmatrix}.$$

Therefore, (4.17) is equivalent to

$$\mathbf{b}_1 \partial_{x_1} \sigma + \mathbf{b}_2 \partial_{x_2} \sigma + B_1 V = g \tag{4.33}$$

with

$$\mathbf{b}_1 = \begin{pmatrix} b_{11} \\ b_{12} \\ 0 \\ b_{14} \\ b_{15} \end{pmatrix} \equiv \begin{pmatrix} \rho v_1 - \rho_0 v_{10} \\ a_{12} - v_1 a_{11} \\ 0 \\ -\rho_0 v_{10} v_{30} \\ a_{15} - (E - v_1^2 + p/\rho) a_{11} - v_1 a_{12} \end{pmatrix}, \quad \mathbf{b}_2 = \begin{pmatrix} 0 \\ 0 \\ p - p_0 \\ 0 \\ 0 \end{pmatrix},$$

and 5×5 matrix B_1 is:

$$B_1 \equiv \begin{pmatrix} \lambda v_1/a^2 & \lambda\rho & 0 & -\rho & 0 \\ \lambda & \lambda\rho v_1 & 0 & 0 & 0 \\ 0 & 0 & \lambda\rho v_1 & 0 & 0 \\ -1 & 0 & 0 & \lambda\rho v_1 & 0 \\ 0 & 0 & 0 & 0 & \lambda\rho v_1 T \end{pmatrix}. \tag{4.34}$$

Here in computing B_1, we have made use of the fact that the flow satisfies system (1.2) behind the shock front.

4.2 Case I: $s \neq \lambda a^{-1}\mu$

Consider the five vectors $(B_1\alpha_1, B_1\alpha_2, B_1\alpha_3, B_1\alpha_4)$ and $s\mathbf{b}_1 + i\omega\mathbf{b}_2$, where B_1 and $\mathbf{b}_j$ are defined as above.

- Vector $B_1\alpha_1 = (\lambda\rho, \lambda\rho v_1, 0, 0, 0)^T$ is parallel to, and hence can be replaced by
$$\zeta_1 = (1, v_1, 0, 0, 0)^T$$
- Vector $B_1\alpha_2 = (i\omega\lambda\rho, 0, s\lambda\rho v_1, -i\omega\lambda^2\rho v_1, 0)^T$ is parallel to
$$\zeta_2 = (i\omega, 0, sv_1, -i\omega\lambda v_1, 0)^T.$$
- Vector $B_1\alpha_3 = (0, 0, 0, 0, \lambda\rho v_1 T)^T$ is parallel to
$$\zeta_3 = (0, 0, 0, 0, 1)^T,$$
- Vector $B_1\alpha_4 = (-\rho\mu\nu^2/a^3, 0, i\omega\lambda\rho v_1\nu^2/a^2, s\rho v_1\nu^2/a^2, 0)^T$ is parallel to
$$\zeta_4 = \left(-a^{-1}\mu, 0, i\omega\lambda v_1, sv_1, 0\right)^T.$$
- Vector $s\mathbf{b}_1 + i\omega\mathbf{b}_2 \equiv \zeta_5$ can be simplified by using Rankine-Hugoniot relations satisfied by the states U_0 and U_1:
$$\begin{cases} \lambda(\rho v_1 - \rho_0 v_{10}) + \rho_0 v_{30} = 0, \\ \lambda(\rho v_1^2 + p - \rho_0 v_{10}^2 - p_0) + \rho_0 v_{10} v_{30} = 0, \\ \lambda\rho_0 v_{10} v_{30} + (p - \rho_0 v_{30}^2 - p_0) = 0 \\ \lambda((\rho E + p)v_1 - (\rho_0 E_0 + p_0)v_{10}) + (\rho_0 E_0 + p_0)v_{30} = 0. \end{cases} \tag{4.35}$$

  Solving $p - p_0$ from the third equation in (4.35)
$$p - p_0 = -\lambda\rho_0 v_{10} v_{30} + \rho_0 v_{30}^2 = \rho_0 v_{30}(v_{30} - \lambda v_{10})$$
  and substituting it into the second equation in (4.35), we obtain
$$\lambda(\rho v_1^2 - \rho_0 v_{10}^2 + \rho_0 v_{30}(v_{30} - \lambda v_{10})) + \rho_0 v_{10} v_{30} = 0,$$
  which simplifies to
$$\lambda\rho v_1^2 = \rho_0(v_{10} + \lambda v_{30})(\lambda v_{10} - v_{30}).$$

From the first equation in (4.32), we obtain

$$\lambda\rho v_1 = \rho_0(\lambda v_{10} - v_{30}).$$

Combining the two relations above, we obtain

$$v_1 = v_{10} + \lambda v_{30}.$$

Therefore, we have

$$\rho_0 v_{10} = \frac{\rho_0 + \lambda^2\rho}{1+\lambda^2}v_1, \quad \rho_0 v_{30} = \frac{\lambda(\rho_0 - \rho)}{1+\lambda^2}v_1.$$

Consequently we obtain

$$\begin{cases} \rho v_1 - \rho_0 v_{10} = \dfrac{\rho - \rho_0}{1+\lambda^2}v_1 \\ \rho v_1^2 - \rho_0 v_{10}^2 + p - p_0 = \dfrac{(\rho-\rho_0)(\rho_0+\lambda^2\rho)}{\rho_0(1+\lambda^2)^2}v_1^2 \\ p - p_0 = \dfrac{\lambda^2 v_1^2}{1+\lambda^2}\dfrac{\rho(\rho-\rho_0)}{\rho_0} = \dfrac{\rho(\rho-\rho_0)}{\rho_0}v_n^2 \\ -\rho_0 v_{10}v_{30} = \dfrac{\lambda(\rho-\rho_0)(\rho_0+\lambda^2\rho)}{\rho_0(1+\lambda^2)^2}v_1^2. \end{cases} \tag{4.36}$$

Therefore we obtain ζ_5

$$\zeta_5 = \begin{pmatrix} s\dfrac{\rho-\rho_0}{1+\lambda^2}v_1 \\ s\dfrac{(\rho-\rho_0)^2 v_1^2\lambda^2}{\rho_0(1+\lambda^2)^2} \\ i\omega\dfrac{\lambda^2 v_1^2}{1+\lambda^2}\dfrac{\rho(\rho-\rho_0)}{\rho_0} = \dfrac{\rho(\rho-\rho_0)}{\rho_0}v_n^2 \\ s\dfrac{\lambda(\rho-\rho_0)(\rho_0+\lambda^2\rho)}{\rho_0(1+\lambda^2)^2}v_1^2 \\ sb_{15} \end{pmatrix} \tag{4.37}$$

where b_{15} can be computed from Rankine-Hugoniot condition:

$$b_{15} = -\frac{(\rho-\rho_0)^2 v_1^3\lambda^2}{\rho_0(1+\lambda^2)^2}.$$

It will be obvious in the following that the explicit form of b_{15} is of no importance. Hence $\zeta_5 =$ is parallel to

$$\big(s(1+\lambda^2)\rho_0, s(\rho-\rho_0)\lambda^2 v_1, i\omega(1+\lambda^2)\lambda^2\rho v_1, s\lambda(\rho_0+\lambda^2\rho)v_1, -s(\rho-\rho_0)\lambda^2 v_1^2\big)^T.$$

Kreiss' condition states that the oblique steady shock front is linearly stable if five vectors $\zeta_1, \zeta_2, \zeta_3, \zeta_4, \zeta_5$ are linearly independent, or the following matrix with these five vectors as column vectors is uniformly non-degenerate on $|s|^2+|\omega|^2=1$, $\eta>0$:

$$\begin{pmatrix} 1 & i\omega & 0 & -a^{-1}\mu & s(1+\lambda^2)\rho_0 \\ v_1 & 0 & 0 & 0 & s(\rho-\rho_0)\lambda^2 v_1 \\ 0 & sv_1 & 0 & i\omega\lambda v_1 & i\omega(1+\lambda^2)\lambda^2\rho v_1 \\ 0 & -i\omega\lambda v_1 & 0 & sv_1 & s\lambda(\rho_0+\lambda^2\rho)v_1 \\ 0 & 0 & 1 & 0 & -s(\rho-\rho_0)\lambda^2 v_1^2 \end{pmatrix} \tag{4.38}$$

Obviously, it is non-degenerate if and only if the following 4×4 matrix J is non-degenerate:

$$J = \begin{pmatrix} 1 & i\omega & -\mu & s(1+\lambda^2)\rho_0 \\ 1 & 0 & 0 & s(\rho-\rho_0)\lambda^2 \\ 0 & s & i\omega\lambda a & i\omega(1+\lambda^2)\lambda^2\rho \\ 0 & -i\omega\lambda & sa & s\lambda(\rho_0+\lambda^2\rho) \end{pmatrix} \tag{4.39}$$

Compute the determinant of J

$$\begin{aligned} \det J = {} & s^3 a(\lambda^2\rho-\rho_0-2\lambda^2\rho_0) - sa\omega^2\lambda^2(1+\lambda^2)(\rho-2\rho_0) \\ & -\lambda\mu[s^2(\rho_0+\lambda^2\rho)-\omega^2(1+\lambda^2)\lambda^2\rho]. \end{aligned} \tag{4.40}$$

We have the following lemma:

Lemma 4.1 Under the condition (4.25), there exists an $\epsilon>0$ such that for all (s,ω) with $s\neq\lambda a^{-1}\mu$

$$|\det J|\geq\epsilon,\ \ \forall |s|^2+|\omega|^2=1,\ \eta=\mathrm{Re}s>0 \tag{4.41}$$

Proof: Noticing that (4.40) is exactly (4.20) in [19], we can copy the proof following (4.20) in [19]. We omit the details here and refer the reader to [19].

4.3 Case II: $s = \lambda a^{-1}\mu$

In the case $s = \lambda a^{-1}\mu$, we have $s = \lambda\omega > 0$ and $\mu = \omega a > 0$. Since

$$s\lambda^2\rho v_1\left(1 - \frac{v_1^2}{a^2}\right) - \xi_1 = -s\rho v_1,$$

$$N(s, i\omega) - \xi_1 I = \begin{pmatrix} -s\rho v_1 & 0 & -i\omega(\lambda\rho v_1)^2 & -s\lambda(\rho v_1)^2 & 0 \\ s & 0 & i\omega\lambda^2\rho v_1 & s\lambda\rho v_1 & 0 \\ i\omega\nu^2/a^2 & 0 & 0 & 0 & 0 \\ s\lambda(1 - \frac{v_1^2}{a^2}) & 0 & -i\omega\lambda\rho v_1 & -s\rho v_1 & 0 \\ 0 & 0 & 0 & 0 & 0 \end{pmatrix}. \quad (4.42)$$

At the point $s = \lambda a^{-1}\mu$, the vectors α_2 in (4.29) and α_4 in (4.30) are parallel, and there are only three linearly independent eigenvectors corresponding the eigenvalue ξ_1:

$$\begin{cases} \alpha_1 = (0, 1, 0, 0, 0)^T, \\ \alpha_2 = (0, 0, 1, -i, 0)^T, \\ \alpha_3 = (0, 0, 0, 0, 1)^T. \end{cases} \quad (4.43)$$

A generalized eigenvector α_4' corresponding to ξ_1 can be found by solving the equation $(N(s, i\omega) - \xi_1 I)\alpha_4' = \alpha_2$, i.e.,

$$\begin{cases} a^2\eta_1 + \lambda\rho v_1(i\eta_3 + \eta_4) = 0, \\ a^2\eta_1 + \lambda\rho v_1(i\eta_3 + \eta_4) = 0, \\ i\nu^2\eta_1 = 1, \\ \lambda^2(a^2 - v_1^2)\eta_1 - \lambda\rho v_1(i\eta_3 + \eta_4) = -i. \end{cases} \quad (4.44)$$

System (4.44) is solvable and has a solution of generalized eigenvector

$$\alpha_4' = (-ia^2\omega^{-1}\nu^{-2}, 0, a^2(\lambda\omega\rho v_1)^{-1}\nu^{-2}, 0, 0)^T,$$

which is parallel to

$$(\lambda\rho v_1, 0, i, 0, 0)^T.$$

Computing $B_1\alpha_1, B_1\alpha_2, B_1\alpha_3, B_1\alpha_4'$ and $s\mathbf{b}_1 + i\omega\mathbf{b}_2$ at $s = \lambda a^{-1}\mu$, we obtain the matrix corresponding to (4.38) as follows

$$\begin{pmatrix} 1 & i\omega & 0 & \lambda^2\rho v_1^2 a^{-2} & s(1+\lambda^2)\rho_0 \\ v_1 & 0 & 0 & \lambda^2\rho v_1 & s(\rho - \rho_0)\lambda^2 v_1 \\ 0 & sv_1 & 0 & i\lambda\rho v_1 & i\omega(1+\lambda^2)\lambda^2\rho v_1 \\ 0 & -i\omega\lambda v_1 & 0 & -\lambda\rho v_1 & s\lambda(\rho_0 + \lambda^2\rho)v_1 \\ 0 & 0 & 1 & 0 & -s(\rho - \rho_0)\lambda^2 v_1^2 \end{pmatrix} \quad (4.45)$$

which is non-degenerate if and only if

$$\det \begin{pmatrix} 1 & i\omega & \lambda^2 \rho v_1^2 a^{-2} & s(1+\lambda^2)\rho_0 \\ v_1 & 0 & \lambda^2 \rho v_1 & s(\rho - \rho_0)\lambda^2 v_1 \\ 0 & s v_1 & i\lambda\rho v_1 & i\omega(1+\lambda^2)\lambda^2 \rho v_1 \\ 0 & -i\omega\lambda v_1 & -\lambda\rho v_1 & s\lambda(\rho_0 + \lambda^2 \rho) v_1 \end{pmatrix} \neq 0,$$

i.e.,

$$\det J' \equiv \det \begin{pmatrix} 1 & -1 & \lambda^2 v_1^2 a^{-2} & (1+\lambda^2)\rho_0 \\ 1 & 0 & \lambda^2 & (\rho - \rho_0)\lambda^2 \\ 0 & 1 & 1 & (1+\lambda^2)\rho \\ 0 & 1 & -1 & (\rho_0 + \lambda^2 \rho) \end{pmatrix} \neq 0. \tag{4.46}$$

It is readily checked that

$$\det J' = (\rho - \rho_0)\nu^2/a^2 + 2(\rho + \rho_0) + \lambda^2(3\rho + \rho_0) > 0.$$

This completes the proof for the case $s = \lambda a^{-1}\mu$. The proof of Theorem 4.1 and hence Theorem 2.1 is complete.

References

[1] G. Ben-Dor, Shock wave reflection phenomena, Springer-Verlag, New York 1992.

[2] S. Canic, B. Keyfitz, and E. H. Kim, Free boundary problems for the unsteady transonic small disturbance equation: transonic regular reflection, Method Appl. Anal. 7(2000), 313–335.

[3] S. Canic, B. Keyfitz, and E. H. Kim, A free boundary problem for a quasi-linear degenerate elliptic equation: Regular reflection of weak shocks, Comm. Pure Appl. Math., LV(2002), 71-92.

[4] G-Q. Chen, Remarks on spherically symmetric solutions of the compressible Euler equations, Proc. Roy. Soc. Edinburgh 127A (1997), 243–259.

[5] G-Q. Chen, M. Feldman, Multidimensional transonic shocks and free boundary problems for nonlinear equations of mixed type, J. Amer. Math. Soc. 16 (2003), no. 3, 461–494.

[6] S-X. Chen, On reflection of multi-dimensional shock front, J. Diff. Eq., 80(1989), 199-236.

[7] S-X. Chen, Existence of local solution to supersonic flow past a three-dimensional wing, Advances in Appl. Math., 13(1992), 273-304.

[8] S-X. Chen, D-N. Li, Supersonic flow past a symmetrically curved cone, Indiana University Mathematics Journal, 49(2000), 1411-1436.

[9] S-X. Chen, Stability of oblique shock front, Sci. China Ser. A, 45(2002), 1012-1019.

[10] S-X. Chen, Z-W. Geng, Z-W and D-N. Li, The existence and stability of conic shock waves, J. Math. Anal. Appl., 277(2003),512-532.

[11] S-X. Chen, D-N. Li, Conical Shock Waves for Isentropic Euler System, (to appear in Proc. Roy. Soc. Edinburgh).

[12] P. Colella, L. F. Henderson, The von Neumann paradox for the diffraction of weak shock waves, J. Fluid Mech. 213 (1990), 71-94.

[13] R. Courant, K. O. Friedrichs, Supersonic Flow and Shock Waves, Interscience Publishers Inc., New York, 1948.

[14] K. O. Friedrichs, Symmetric positive linear differential equations, Comm. Pure Appl. Math., 11(1958), 333-418.

[15] H. Hornung, Regular and Mach reflection of shock waves, Ann. Rev. Fluid Mech., 18(1986), 33-58.

[16] Kreiss, H-O., Initial Boundary value problems for hyperbolic systems, Comm. Pure Appl. Math., 23(1970), 277-298.

[17] P. D. Lax, R. S. Phillips, Local boundary conditions for dissipative symmetric linear differential operators, Comm. Pure Appl. Math. 13(1960), 427–455.

[18] D-N. Li, Rarefaction and shock waves for multi-dimensional hyperbolic conservation laws, Comm. P. D. E. 16(1991), 425-450.

[19] D-N. Li, Analysis on linear stability of oblique shock waves in steady supersonic flow, J. Diff. Eq., 207(2004), 195-225.

[20] Lien, W-C. and Liu, T-P., Nonlinear stability of a self-similar 3-D gas flow, Comm. Math. Phys. 304(1999) 524-549.

[21] A. Majda, The stability of multi-dimensional shock fronts, Memoir Amer. Math. Soc. 273(1983).

[22] A. Majda, Compressible fluid flow and systems of conservation laws in several space variables, Springer-Verlag, New York, 1984.

[23] G. Metivier, The block structure condition for symmetric hyperbolic systems, Bull. London Math. Soc. 32 (2000), no. 6, 689–702.

[24] G. Metivier, Stability of multidimensional shocks, Advances in the Theory of Shock Waves, 25-103. Birkhauser Boston, Boston, 2001.

[25] C. S. Morawetz, Potential theory for regular and Mach reflection of a shock at a wedge, Comm. Pure Appl. Math. 47 (1994),593–624.

[26] J. Rauch, Symmetric positive systems with boundary characteristic of constant multiplicity, Trans. Amer. Math. Soc. 291(1985), 167-187.

[27] D. G. Schaeffer, Supersonic flow past a nearly straight wedge, Duke Math. J. 43(1976), 637–670.

[28] D. Serre, Systems of conservation laws 2, Cambridge University Press, Cambridge, 2000.

[29] D. Serre, Shock reflection in gas dynamics. To appear in Volume IV of Handbook of Mathematical Fluid Dynamics. S. Friedlander and D. Serre eds. Elsevier, Amsterdam (2006).

[30] J. Smoller, Shock waves and reaction-diffusion equations, Springer-Verlag, New York, 1983.

[31] M. Taylor, Partial Differential Equations, II, Springer, New York, 1997.

[32] V. M. Teshukov, Stability of regular shock wave reflection, J. Appl. Mech. Tech. Phys., 30 (1989), 189-196.

[33] Y-X. Zheng, Existence of solutions to the transonic pressure-gradient equations of the compressible Euler equations in elliptic regions, Comm. Partial Diff. Equ., 22 (1997), 1849-1868.